Materials Advances

ROYAL SOCIETY OF CHEMISTRY

PAPER

View Article Online
View Journal

Cite this: DOI: 10.1039/d5ma01324k

Tuning the mechanical performance of polydicyclopentadiene copolymers through dicyclopentadienone monomer incorporation

Benjamin Godwin,*[a] Adam Sylvain-Stewart[a] and Jeremy E. Wulff *[ab]

Received 14th November 2025,
Accepted 21st March 2026

DOI: 10.1039/d5ma01324k

rsc.li/materials-advances

Engineering plastics are a class of polymer materials with enhanced mechanical and thermal properties. Polydicyclopentadiene (PDCPD) is an emerging example of this class of material derived from petrochemical waste. Herein, we describe the copolymerization of dicyclopentadiene with novel oxadicyclopentadiene monomer to produce mechanically and thermally tunable PDCPD-based materials. We also improve surface functionality while apparently reducing atmospheric oxidation, thereby addressing two major barriers to further adoption of this material.

Introduction

Polydicyclopentadiene (PDCPD) is a thermosetting polymer derived from the ring opening metathesis polymerization (ROMP) of dicyclopentadiene (DCPD).[1,2] PDCPD has significant commercial value owing to its excellent mechanical and thermal properties. It is particularly favored for its impact resistance at both high and low temperatures.[3,4] It also benefits from a reduced carbon footprint, since DCPD is readily available as waste from the C5 fraction of petroleum distillates (where it results from the spontaneous dimerization of cyclopentadiene, following distillation) and as the byproduct of steam cracking of heavy distillates to make ethylene.[1] Additionally, due to the energy contained in the strained norbornene ring of the monomer, the polymerization—and therefore the manufacturing—of PDCPD parts uses substantially less energy than other types of plastics such as polyethylene which requires a high temperature melt before injection molding in expensive high-pressure molds.[2,5,6]

Manufacturing of PDCPD is done through reaction injection molding (RIM).[2] In RIM a resin (mixture of catalyst, monomer(s), inhibitors, additives) is injected into a mold and heated to a moderate temperature.[2] This initial heating prompts the extremely exothermic ROMP reaction with temperatures often exceeding 200 °C spontaneously.[2,5,6] This process requires low pressure molds and little energy input compared to that of typical injection molding, which dramatically reduces tooling and energy costs associated with production.[2] The utility of RIM is a major advantage of PDCPD. RIM is high throughput (a typical cycle takes less than 5 minutes), and very large parts (up to 100 kg) can be made very quickly.[2] Complex geometries are easily incorporated owing to the low viscosity of the resin.[2] Recent advances by the Moore group have also shown that the energy required for PDCPD molding can be lowered even further using frontal polymerization, wherein only a small amount of initial heat is required to start the polymerization reaction.[5–8] The exotherm of the ROMP reaction maintains the heat required for continued polymerization and curing of the final product.[5–8]

While PDCPD has many good qualities, it has poor end-of-life utility owing to the crosslinked matrix that is required for its desirable mechanical and thermal properties.[1,2,9,10] Crosslinked thermosets do not flow when heated, and therefore it is not possible to recycle the material using typical methods.[11] In addition to its lack of end-of-life utility, PDCPD has several other disadvantages that restrict its wider adoption. As the crosslinking and polymerization reactions occur simultaneously, monomer can be trapped in the polymer matrix leading to an unpleasant acrid odor (perceptible at 3–5 ppb).[2,12] Additionally, due to the lack of hetero-atom inclusion, PDCPD is not chemically tunable and has a low surface energy when it is freshly prepared.[2] The low surface energy precludes the use of paints and adhesives without a surface oxidation step. Waiting for the polymer to oxidize bottlenecks the otherwise rapid RIM process.[2] The low polarity of the matrix also results in low interfacial adhesion with commercially available fiber reinforcements with typical (polar) sizing geared towards epoxy and polyester resin systems.[2,13]

In previous work, we and others have shown that many of these disadvantages can be solved by incorporating various functional groups.[12,14–17] Addition of functional groups reduces

[a] Department of Chemistry, University of Victoria, Victoria, British Columbia, V8W 3V6, Canada. E-mail: benjamin.les.godwin@gmail.com, wulff@uvic.ca
[b] Centre for Advanced Materials and Related Technology (CAMTEC), University of Victoria, Victoria, BC, V8W 2Y2, Canada

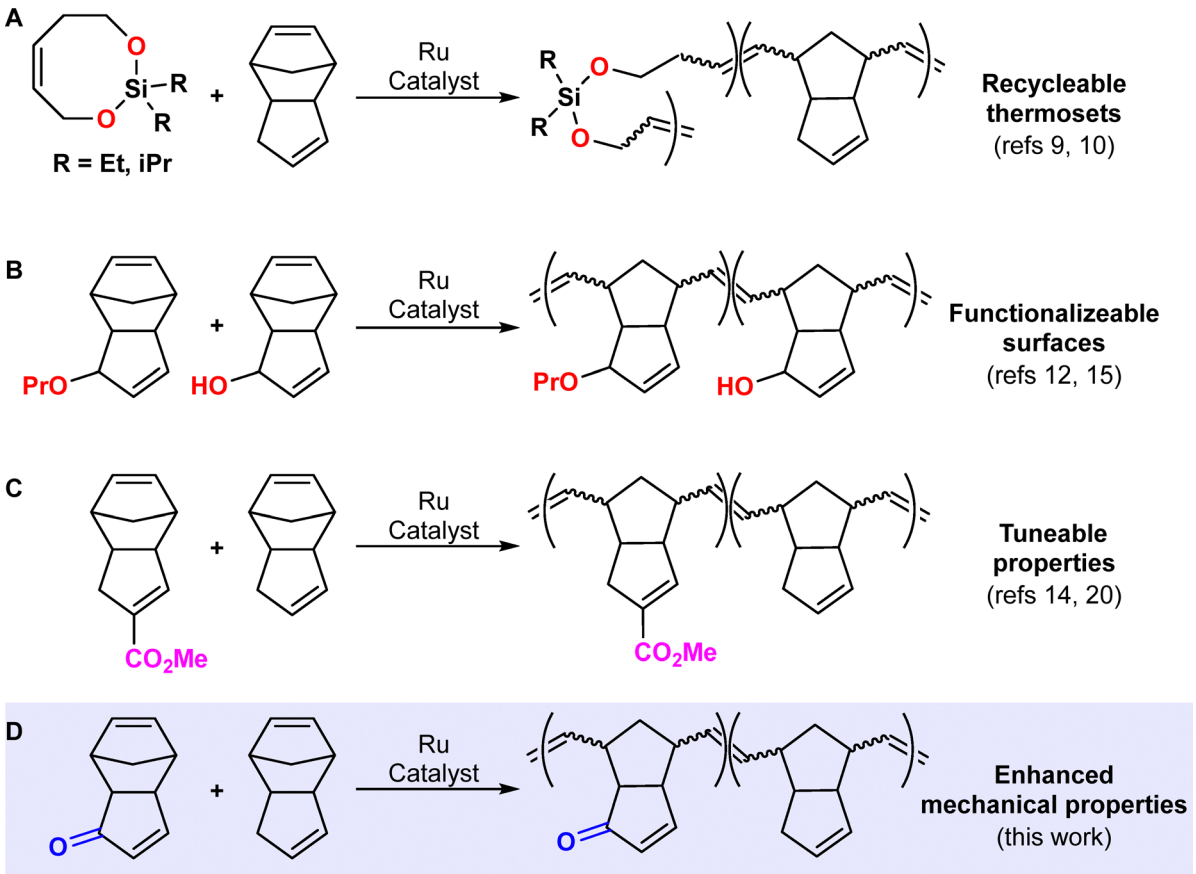

Fig. 1 Recent copolymerization strategies for PDCPD. (A) Degradable thermosets *via* copolymerization with cleavable silyl ethers. (B) Copolymerization of functional DCPD-based monomers leading to tuneable PDCPD materials. (C) Copolymerization of *f*DCPD and DCPD resulting in materials with adaptable and functional surfaces. (D) This work: copolymerization of oxaDCPD and DCPD, to afford materials with enhanced mechanical properties.

the vapor pressure or imparts pleasant odors to the monomer.[12,17,18] The polarity of these included functional groups leads to increased water contact angles and thus greater surface energy upon fresh preparation.[12,14,17,18] Additionally, polymerization of these functional monomers results in enhanced or tunable mechanical properties.[16–18] The challenge and practicality of the installation of such functional groups ranges greatly, but in general leads to a monomer that is significantly more laborious and thus expensive to produce. Copolymerization has arisen as a suitable strategy to combat this challenge.

The Johnson and Moore groups have shown that the inclusion of small amounts of silyl ether species into DCPD resins leads to thermosets that can be degraded into reusable oligomers (Fig. 1A).[9,10] The Xu and the Lemcoff groups each reported the selenium dioxide oxidation of DCPD (Fig. 1B). This preparation is simple to carry out but requires the use of stoichiometric selenium dioxide which has been shown to be toxic. More importantly, the atom economy of this method is poor and not practical for industrial purposes.[12,15] Nevertheless, the allylic alcohol product can be derivatized through esterification or etherification, leading to a diverse range of monomers which all undergo polymerization in the presence of the Grubbs 1st and 2nd generation initiators.[12,15,16] However, the resulting polymers and copolymers all suffer from the thermal lability of allylic functional groups. This leads to facile two-step decomposition above 200 °C observed *via* TGA. Furthermore, these polymers also display glass transition temperatures of <100 °C, which is not practical for current applications of PDCPD.

Our group has pioneered two different approaches to functionalizing DCPD.[17,18] The first-generation, ester-functionalized DCPD (*f*DCPD) utilized a vinyl ester formed through the Diels–Alder reaction of cyclopentadiene and carboxylated cyclopentadiene (Fig. 1C).[18,19] This monomer produced a glassy polymer through reaction injection molding that had similar mechanical and thermal properties to native PDCPD but with the benefit of a fruity ester odor, tunable surface energy, and facile functionalization.[14,18,20] However, significant (1 mol %) quantities of initiator and substantial reaction time were required for polymerization. The production of the *f*DCPD monomer through the Diels–Alder reaction is also not atom economical.

Inspired by the ease of the Xu and Lemcoff approach, we were able to synthesize a much improved second-generation *f*DCPD (oxaDCPD) (Fig. 1D).[17] OxaDCPD is readily synthesized on large (>200 g per batch) scale in the laboratory, and is purified using industrially relevant methods (distillation). We have also shown that oxaDCPD yields a glassy polymer through

reaction injection molding, using modest (0.05 mol%) initiator loadings, and that this glassy polymer exceeds the benchmark mechanical and thermal properties set by the parent PDCPD.[17] Regarding the cost of production, however, oxaDCPD needs to be generated in a separate step, which necessarily increases its cost (and that of the corresponding homopolymer) relative to that of unfunctionalized DCPD (which is a petrochemical waste material).

In the present work, we explore the synthesis of a series of oxaDCPD-*co*-DCPD copolymers, in an effort to benefit from the enhanced properties of oxaDCPD at a practical cost. As part of this study, we aimed to find the minimal required amount of oxaDCPD needed to engender an improvement in thermal and/or mechanical properties.

Here we show the synthesis of eight different oxaDCPD-containing materials and corresponding controls, ranging from pure DCPD to 40% oxaDCPD content. We also explore the effects of adding ethylidene norbornene (ENB), a commonly employed comonomer in academic research of PDCPD.[5,6,21] We assessed each material's tensile strength, toughness, Young's modulus, storage modulus, glass transition temperature and thermal stability through the use of macro-scale regular dimensioned samples accessed through reaction injection molding.

Results and discussion

Copolymers were produced *via* reaction injection molding, which is an industrially relevant production method for

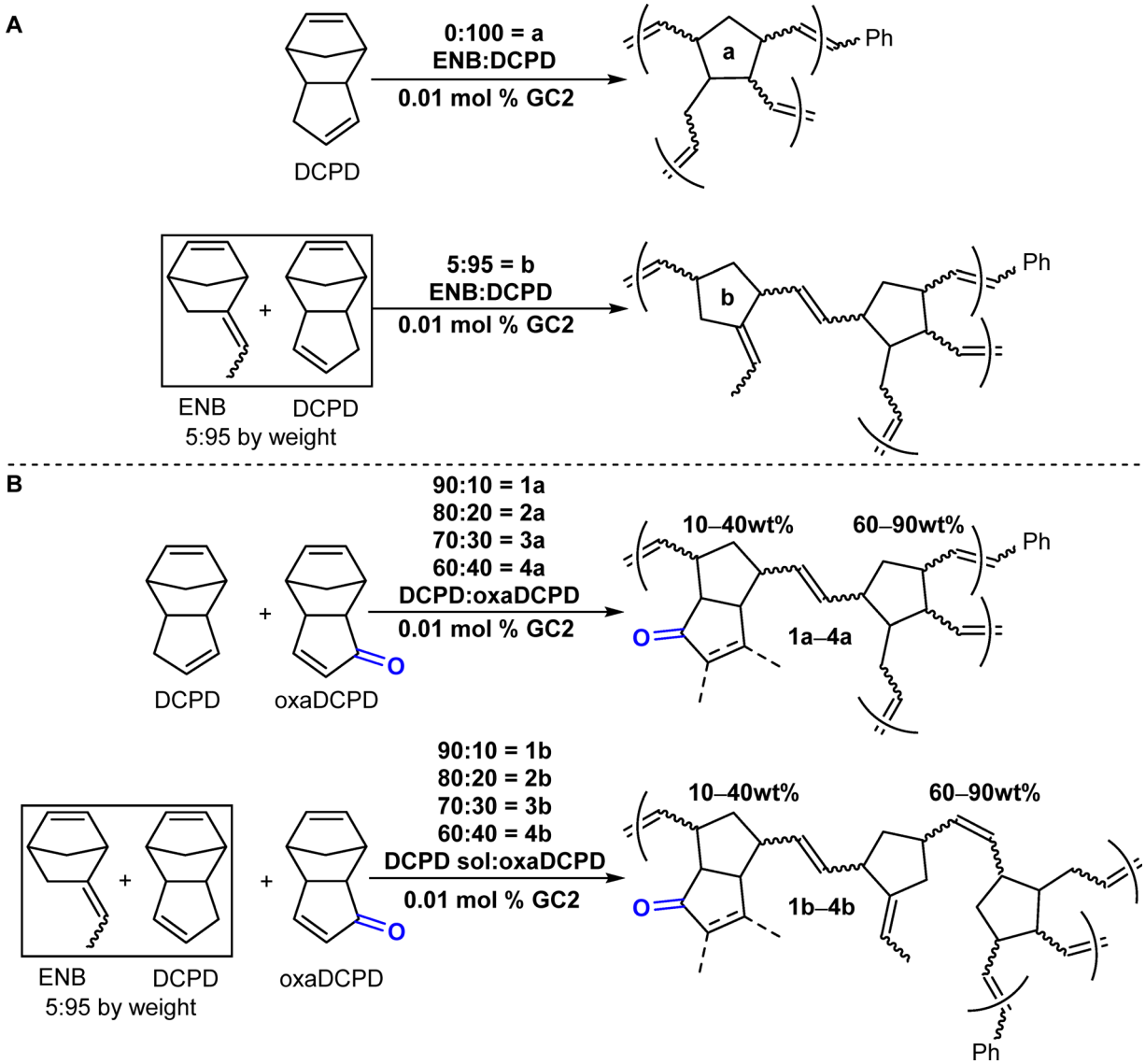

Fig. 2 (A) Synthesis of polydicyclopentadiene controls using Grubbs second generation initiator. Only a fraction of cyclopentene rings within the polymer engage in crosslinking. (B) Synthesis of oxaDCPD-*co*-DCPD copolymers. Monomer ratios refer to weight percent; for mole percent values, refer to Table S1. Wavy bonds are used to indicate mixtures of *E* and *Z* alkenes. Dashed bonds are used to indicate that some percentage of the cyclopentenone groups will engage in thermally initiated radical addition reactions,[17,19] resulting in the presence of inter-chain and intra-chain crosslinks. Similar radical crosslinking reactions will occur at other alkenes in the polymer chain, but these are not shown.

PDCPD-based materials.[1,2,22] We produced two different types of PDCPD-*co*-oxaDCPD copolymers and their respective PDCPD controls: in **type a** copolymers pure DCPD was used as the comonomer; in **type b** copolymers a 95 : 5 solution of DCPD:ENB was used (Fig. 2). This mixture of DCPD and ENB is commonly employed in the existing academic literature as a surrogate to pure DCPD. The addition of ENB depresses the melting point of DCPD (32.5 °C) below room temperature, making it easier to solubilize catalysts and inhibitors, and to enable simple laboratory reaction injection molding by preventing solidification of the resin during injection into a mold. Reaction injection molding of all samples was initiated by adding Grubbs second-generation catalyst (GC2, 0.01 mol%) to a molten combination of monomers as shown in Fig. 2A and B. Additional details are available in the SI.

For all copolymer samples, the label **1**, **2**, **3**, or **4** indicates the use of 10, 20, 30, or 40% oxaDCPD content by weight (mol% values for all formulations are provided in Table S1). Thus, polymer **1a** was formed from 10% oxaDCPD and 90% DCPD, while **1b** was formed from 10% oxaDCPD and 90% of a 95 : 5 mixture of DCPD and ENB. Control samples were also prepared, in which no oxaDCPD was added to the formulation. These samples are represented with an **a** or **b** (indicating the absence or presence of ENB comonomer, respectively) with no preceding number.

In previous work we directly formed appropriately shaped samples for mechanical testing through RIM. However, due to the limitations of lab-scale reaction injection molding, this often leaves voids or other imperfections which leave many samples unusable. To remedy this, we produced rectangular, regular-dimensioned plaques that were then cut by the University of Victoria Science Machine Shop into the desired samples. The advantage to this is two-fold. It avoids wasting novel material on defective samples, and all samples are produced identically without any inconsistencies in surface- or edge-smoothness. Two plaques of each copolymer were produced; one plaque was used to produce dogbones for tensile testing and the other was used to cut samples for DMTA. For assessment of batch-to-batch variability for representative materials, see Fig. S35 in the SI.

Infrared spectroscopy of the freshly exposed surface of the reaction injection molded materials showed an increasing intensity of carbonyl stretch at *ca.* 1707 cm^{-1} in copolymers with increasing oxaDCPD content (Fig. S4 and S7). There did not appear to be a difference in the presence of surface functionality between the **a** or **b** stream of copolymers. As expected, the freshly exposed surface of both PDCPD controls did not show any signals in the 3000–3300 cm^{-1} or 1700 cm^{-1} regions, corresponding to hydroxyl or carbonyl functional groups. In contrast, samples exposed to air for greater than 24 hours after manufacturing showed both hydroxyl and carbonyl surface functionality (Fig. S3 and S6). After heating during dynamic mechanical thermal analysis (DMTA, refer to the SI for a detailed description of the heat treatment), PDCPD homopolymer samples showed higher intensities of hydroxyl surface functionality and (perhaps most dramatically) carbonyl functionality than did unheated PDCPD samples (black spectral traces in Fig. 3A and B). Interestingly, however, increasing the oxaDCPD content showed that some copolymers were able to resist the formation of surface hydroxyl groups and, at least for **2a–4a**, also resist the apparent formation of new carbonyl functionality.

The lack of surface functionality for freshly prepared PDCPD surfaces and over-oxidation upon exposure to air (resulting in

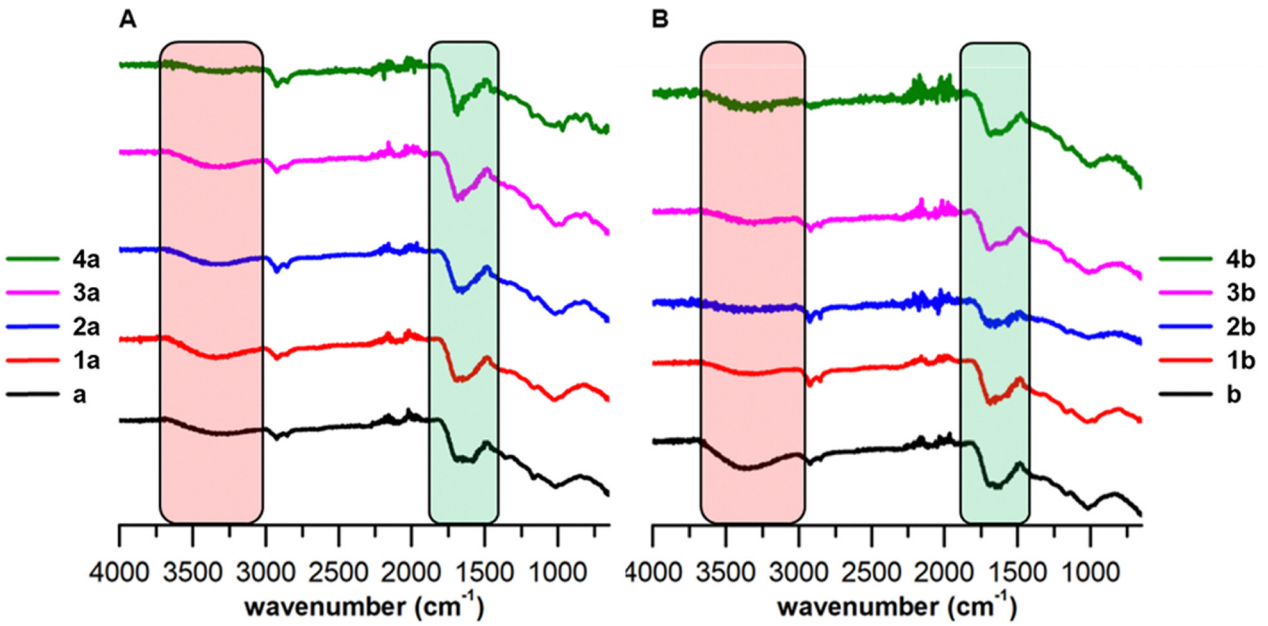

Fig. 3 (A) ATIR spectra of **a type** polymers after controlled heating during DMTA (see the SI for precise heating parameters). (B) ATIR spectra of **b type** polymers after heating during DMTA.

autoxidation) are both major problems industrially.[2] Parts must be left to oxidize before painting or bonding can be performed, since a lack of surface energy prevents adhesives and coatings from sticking.[2] On the other hand, too much surface oxidation leads to oxidative embrittlement and can reduce impact resistance, one of PDCPD's most prized characteristics.[23] The apparent resistance of some of the copolymers to thermally induced oxidation, while simultaneously presenting a controllably functionalized surface, could be very advantageous to industry, offering decreased production times and potentially more robust materials.

Both classes of copolymers and control PDCPD polymers swell dramatically (~200% of initial mass) in toluene, and all materials started to experience mass loss after 2 days of solvent exposure (Fig. S32). The incorporation of polar oxaDCPD monomer into the copolymers did not seem to significantly increase the uptake of methanol as compared to neat samples of oxaDCPD prepared in previous work.[17]

We interrogated the mechanical properties of the materials using dynamic mechanical thermal analysis (DMTA) and tensile testing (TT). Young's modulus, ultimate tensile strength and toughness were assessed through tensile testing. The

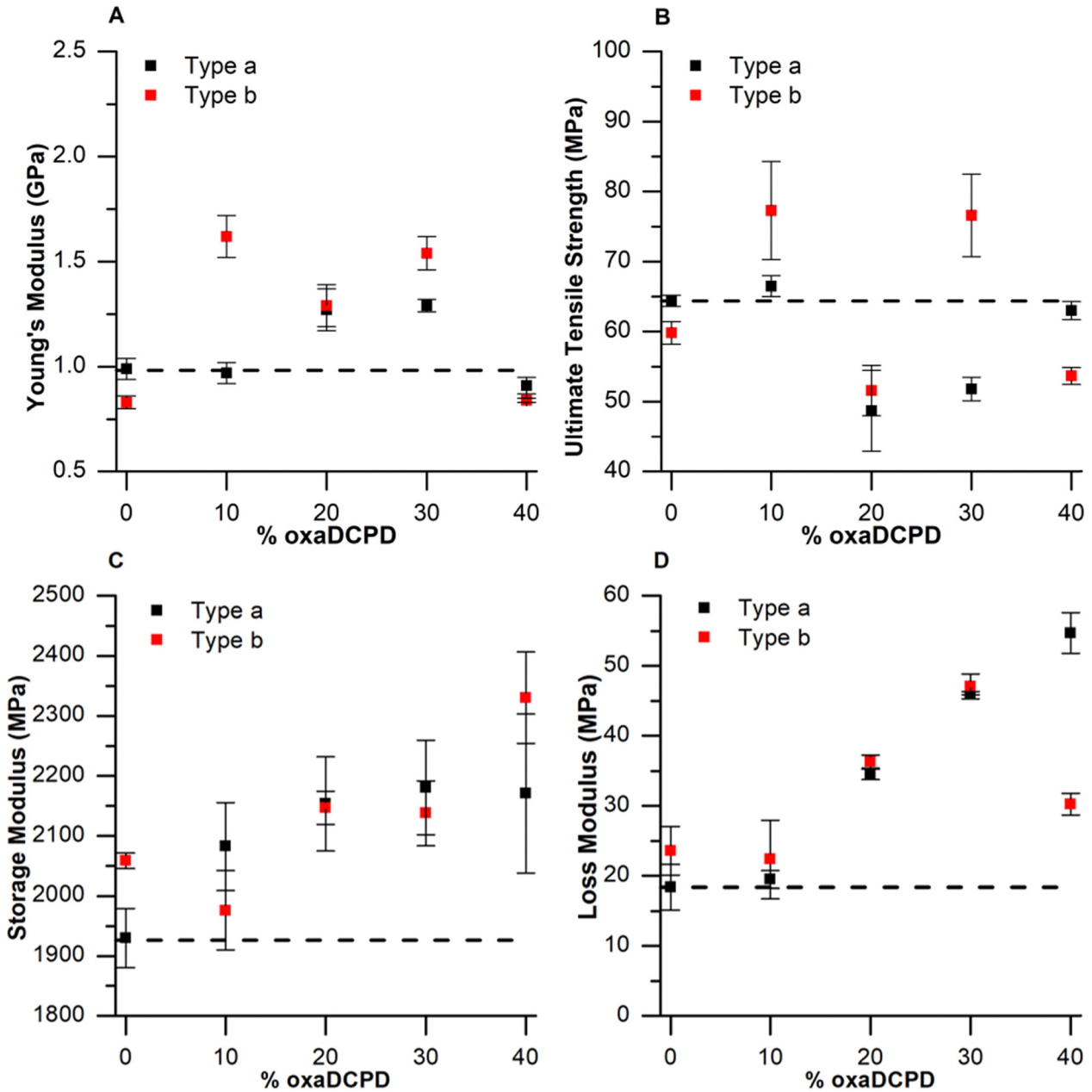

Fig. 4 Mechanical properties of copolymers and corresponding PDCPD controls. (A) Young's modulus. (B) Ultimate tensile strength. (C) Storage modulus. (D) Loss modulus. Data for panels A and B were obtained using ASTM d638 type V dogbone samples. Data for panels C and D were obtained using 25 × 10 × 3 mm bar samples. Error bars represent standard deviation of at least n = 3 replicates.

results are summarized in Fig. 4A and B and Table S2. The increase in Young's modulus was consistently higher in **type b** samples and was highest overall for **1b**. The ultimate tensile strength of **type b** copolymers fluctuated greatly with increasing volume fraction of oxaDCPD. Similarly, **type a** copolymers also fluctuated with oxaDCPD content, with **1a** having the highest ultimate tensile strength of **type a** polymers. Modulus of toughness was calculated from the area under the curve of the tensile stress–strain curve (as shown in the selected stress–strain plots in Fig. 5). All **type b** samples except for **4b** had increased modulus of toughness compared with the native **b** polymer. Copolymers **1b** and **3b** showed the greatest increases in modulus of toughness. Samples **1a**, and **4a** had similar modulus of toughness as the **type a** homopolymer, whilst **2a** and **3a** exhibited lower toughness.

We further assessed our copolymers' resistance to plastic deformation utilizing Vickers Hardness (VH) testing.[24] Hardness testing allows for many measurements when using scarce materials—such as a novel monomer like oxaDCPD—because the test does not require any special sample geometry. The lack of specific sample geometry is also useful as it makes the test at least somewhat immune to defects which are easy to introduce into larger, more precise samples. These defects can result in stress concentrations giving variable results. Similarly to tensile testing, the hardness measurement is a measure of a material's resistance to plastic deformation and thus a comparison to tensile strength may be established.[24–26] VH testing confirmed the nonmonotonic relationship found in the tensile testing; data are summarized in Table S3 and in Fig. S34 of the SI.

The nonmonotonic differences between each copolymer and the variability in toughness may arise from the fact that the oxaDCPD monomer polymerizes more slowly than the native DCPD monomer.[27] The reduction in reactivity is likely caused by temporary inhibition of the metathesis catalyst through the formation of a known oxygen chelate species,[28,29] and may lead in turn to the generation of a gradient copolymer. A heterogeneous distribution of polar ketone groups within the bulk material would naturally lead to higher local concentrations of crosslinking density through the non-canonical hydrogen bonding interaction between the ketone and beta-hydrogen (Fig. 6).[17,30–32] The size and morphology of these zones likely also fluctuates with the volume fraction of oxaDCPD added, through concentration-dependent aggregation, crystallization and packing effects.[33,34]

The storage modulus and loss modulus were obtained *via* DMTA. The results are summarized in Fig. 4C, D and Table S2. The storage modulus increased with the addition of oxaDCPD content for both **type a** and **type b** copolymers, except for **1b** which saw a decrease in storage modulus. The loss modulus also followed a similar trend, increasing in a linear fashion from oxaDCPD fractions of 10% onward, except for **4b** which saw a sharp drop in loss modulus. Interestingly, **1a** and **1b** did not show substantive increases in loss modulus like all other measured mechanical parameters. Instead, **1a** and **1b** had similar values of loss modulus compared to the native polymers **a** and **b** respectively. The maintenance and increase of the storage modulus in both classes of copolymers is of great significance, since PDCPD is an engineering plastic.[2,4] The

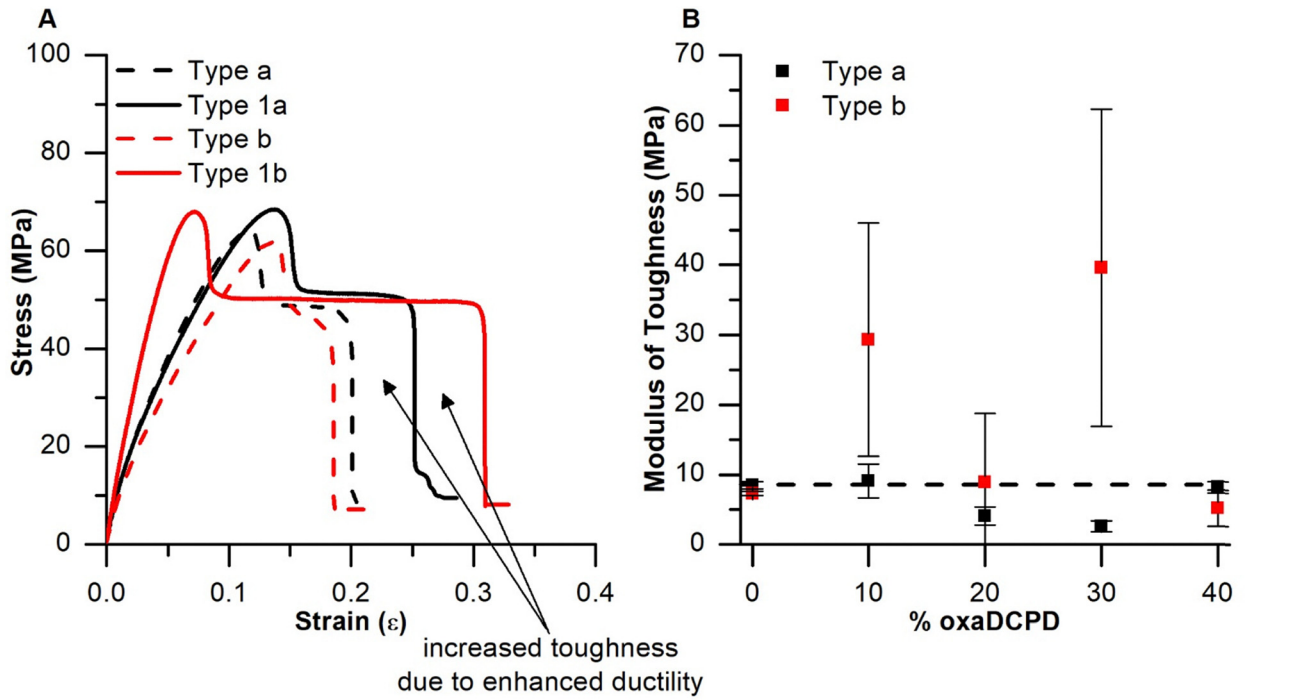

Fig. 5 (A) Select tensile plots demonstrating increased toughness in the stress–strain curve. (B) Modulus of toughness of copolymers and corresponding PDCPD controls. Data were obtained through tensile testing, using ASTM d638 type V dogbone samples. Error bars represent standard deviation of $n = 3$ for all samples.

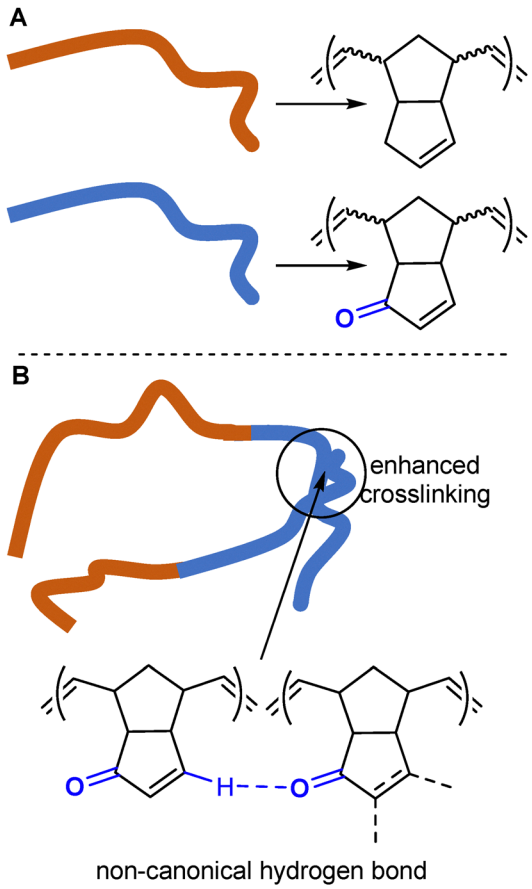

Fig. 6 (A) Cartoon depictions of PDCPD and oxaPDCPD. (B) Non-canonical hydrogen bonding in regions containing high local concentrations of cyclopentenone substituents within a gradient copolymer.

ability to increase and tune both the stiffness and damping ability of the material could be valuable when designing automotive parts. By adding small amounts of oxaDCPD we can access a material that is stronger, stiffer, more damping, and tougher than regular PDCPD. This could offer significant advantages, allowing automotive parts to be thinner and lighter—improving fuel economy while maintaining the required strength.

We investigated the thermal properties of the new materials *via* DMTA, differential scanning calorimetry (DSC), and thermogravimetric analysis (TGA). The results are summarized in Fig. 7 and Table S1, Fig. S9–11, and S33; refer to the SI for detailed experimental parameters. The glass transition temperatures (T_g) were derived from the peak of the loss factor obtained through DMTA and further supported by DSC (see Table S1 and Fig. S9–11). The T_g of copolymer **1a** was the highest of the copolymers, and was comparable to that of polymer **a**: 186.0 °C *vs.* 186.1 °C. T_g values for **2a–4a** were all substantially lower than those for **1a**. We have previously shown that a high concentration of the slower-reacting oxaDCPD monomer reduces the polymerization temperature in reaction injection molding trials, by slowing down the rate at which energy is released from the strained alkene.[27] For copolymers **2a–4a**, this reduced polymerization temperature likely results in

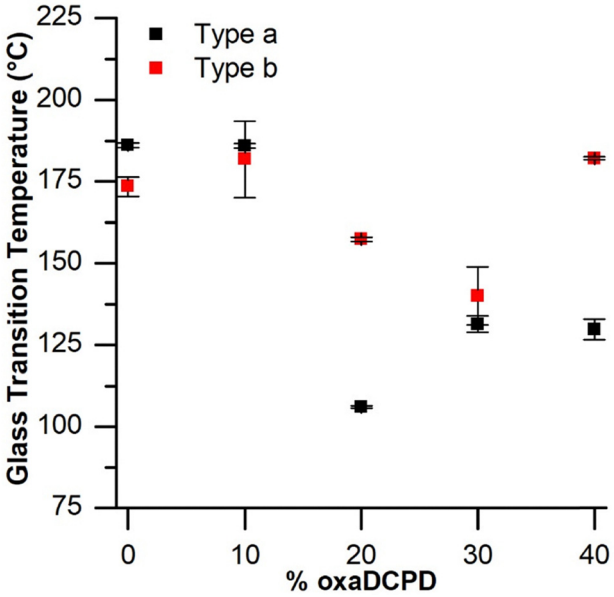

Fig. 7 Glass transition temperatures of copolymers and corresponding PDCPD controls derived from the peak of the loss factor from DMTA experiments. Error bars represent standard deviation of n = 3 for all samples.

the formation of shorter-chain oligomers, which in turn depress the glass transition temperature.

T_g values for **b** and **1b** were slightly lower than those for **a** and **1a**—likely due to the fact that ENB acts as a chain extender during the polymerization, reducing the crosslinking density.[17,35] This results in a lowered T_g value as compared to the **a type** homopolymer and **1a** copolymer. At the same time, however, the presence of the fast-reacting ENB comonomer assists in maintaining a high temperature in the reaction injection molding protocol. This helps to counteract the depressive effect of high oxaDCPD concentrations on the T_g, meaning that the glass transition temperatures for **2b**, **3b**, and **4b** all exceed those for **2a**, **3a**, and **4a**.

Thermogravimetric analysis of samples **a**, **b**, **1a**, **1b**, **2b**, **3a**, **3b** and **4b** showed <10% mass loss up to 400 °C, indicating that no thermally labile groups are introduced during the copolymerization process (Fig. S33). However, all materials made with ≥20% oxaDCPD showed small mass reductions at 300 °C—probably due to loss of low molecular weight oligomers, as discussed above—but did not degrade beyond *ca.* 15% mass loss until reaching temperatures of approximately 450 °C. In keeping with the T_g results, the presence of ENB in the monomer mixture (which helps to maintain a high reaction temperature throughout the polymerization,[27] thereby minimizing the presence of oligomers) resulted in reduced mass loss for high oxaDCPD materials **3b** and **4b**, relative to **3a** and **4a**.

Conclusion

We manufactured eight novel PDPCD-based copolymers using reaction injection molding, utilizing the easily accessible and

scalable functional DCPD monomer oxaDCPD. We have shown that the addition of a small amount of this material to DCPD-based resins has a remarkable effect on the mechanical, chemical, and thermal properties of the resulting materials. We show that the tensile strength, Young's modulus, storage modulus, loss modulus, toughness, and glass transition temperature can all be improved and/or tuned by utilizing oxaDCPD as a comonomer. We also showed—through a qualitative FTIR study—the potential for resistance to surface autoxidation (a property known to be related to material embrittlement[2,23,36]) through the incorporation of oxaDCPD into the material. Precise quantitative assessment of surface oxidation was complicated by the fact that addition of the ketone-containing monomer naturally increases total elemental oxygen concentration within the bulk material, however, and further study will be needed to define the precise consequences of this effect, in terms of long-term mechanical performance.

In addition to the modulus changes noted above, the surface of the freshly prepared copolymer is naturally functionalized with polar ketone groups, and we have previously shown a reduction in water contact angle (relative to that of the PDCPD homopolymer) through incorporation of the oxaDCPD monomer.[17] The presence of such polar groups (without the need for secondary surface-ageing steps that are time-consuming, and which may yield inconsistent results) potentially enables faster production of parts that need to be painted or treated with various coatings. All of these properties are core to PDCPD's use as an engineering plastic on heavy machinery, and as a structural material.[2,4,13] The ability to improve these properties enables less material to be used to fulfill existing uses and may lead to further applications in niche markets like the aerospace industry that demand significantly more from materials.[2,4,13]

Author contributions

The manuscript was written through contributions of all authors. All authors have given approval to the final version of the manuscript.

Conflicts of interest

The authors declare the following competing financial interest: B. G. and J. W. are co-inventors on US20240308939A1, which claims the use of the copolymers described herein. There are no addition conflicts to declare.

Data availability

The data supporting the findings of this study are available within the article and its supplementary information (SI). Supplementary information: complete experimental details, spectra for all new compounds, supplemental tables and figures. See DOI: https://doi.org/10.1039/d5ma01324k.

Acknowledgements

The authors thank Sean Adams, Chris Secord and Kody Matthews for their contributions to the creation of the photochemical reactor. In addition, we further thank Chris Secord and Kody Matthews for the creation of the reaction injection molding apparatus and for cutting samples. We also thank Ryan Mandau at the University of British Columbia Okanagan Campus Survive and Thrive Applied Research Laboratory for Vickers microhardness measurements. The authors acknowledge and thank the Innovation for Defence Excellence and Security (IDEaS) Program of the Canadian Department of National Defence (project IDEaS-4-1a-CP4-0299) for operating funds that were used to support this research. Additional financial support was provided by the Natural Sciences and Engineering Research Council of Canada (NSERC) through a Discovery grant to J.W.

References

1 S. Kovačič and C. Slugovc, *Mater. Chem. Front.*, 2020, **4**, 2235–2255.
2 D. Vervacke, An Introduction to PDCPD: Poly-Di-Cyclo-Penta-Diene, Product Rescue, 2008.
3 Q. Beuguel, E. Kirillov, J.-F. Carpentier and S. M. Guillaume, *ACS Appl. Polym. Mater.*, 2022, **4**, 2251–2255.
4 P. Y. Le Gac, D. Choqueuse, M. Paris, G. Recher, C. Zimmer and D. Melot, *Polym. Degrad. Stab.*, 2013, **98**, 809–817.
5 D. Robertson, M. Yourdkhani, P. J. Centellas, J. E. Aw, D. G. Ivanoff, E. Goli, E. M. Lloyd, L. M. Dean, N. R. Sottos, P. H. Geubelle, J. S. Moore and S. R. White, *Nature*, 2018, **557**, 223–227.
6 B. A. Suslick, K. J. Stawiasz, J. E. Paul, N. R. Sottos and J. S. Moore, *Macromolecules*, 2021, **54**, 5117–5123.
7 D. M. Alzate-Sanchez, C. H. Yu, J. J. Lessard, J. E. Paul, N. R. Sottos and J. S. Moore, *Macromolecules*, 2023, **56**, 1527–1533.
8 I. D. Robertson, E. L. Pruitt and J. S. Moore, *ACS Macro Lett.*, 2016, **5**, 593–596.
9 E. M. Lloyd, J. C. Cooper, P. Shieh, D. G. Ivanoff, N. A. Parikh, E. B. Mejia, K. E. L. Husted, L. C. Costa, N. R. Sottos, J. A. Johnson and J. S. Moore, *ACS Appl. Eng. Mater.*, 2023, **1**, 477–485.
10 K. E. L. Husted, C. M. Brown, P. Shieh, I. Kevlishvili, S. L. Kristufek, H. Zafar, J. V. Accardo, J. C. Cooper, R. S. Klausen, H. J. Kulik, J. S. Moore, N. R. Sottos, J. A. Kalow and J. A. Johnson, *J. Am. Chem. Soc.*, 2023, **145**, 1916–1923.
11 W. Post, A. Susa, R. Blaauw, K. Molenveld and R. J. I. Knoop, *Polym. Rev.*, 2020, **60**, 359–388.
12 S. Saha, Y. Ginzburg, I. Rozenberg, O. Iliashevsky, A. Ben-Asuly and N. G. Lemcoff, *Polym. Chem.*, 2016, **7**, 3071–3075.
13 K. A. M. Vallons, R. Drozdzak, M. Charret, S. V. Lomov and I. Verpoest, *Composites, Part A*, 2015, **78**, 191–200.
14 T. Li and J. E. Wulff, *ACS Appl. Polym. Mater.*, 2021, **3**, 110–115.
15 L. Gong, K. Liu, E. Ou, F. Xu, Y. Lu, Z. Wang, T. Gao, Z. Yang and W. Xu, *RSC Adv.*, 2015, **5**, 26185–26188.

16 R. S. Phatake, A. Masarwa, N. G. Lemcoff and O. Reany, *Polym. Chem.*, 2020, **11**, 1742–1751.
17 B. Godwin, M. H. Anvari, T. Olfatbakhsh, M. Mahbod, A. S. Milani, G. A. DiLabio and J. E. Wulff, *Macromolecules*, 2023, **56**, 1592–1600.
18 J. Chen, F. P. Burns, M. G. Moffitt and J. E. Wulff, *ACS Omega*, 2016, **1**, 532–540.
19 T. J. Cuthbert, T. Li, A. W. H. Speed and J. E. Wulff, *Macromolecules*, 2018, **51**, 2038–2047.
20 T. Li, H. Shumka, T. J. Cuthbert, C. Liu and J. E. Wulff, *Mater. Adv.*, 2020, **1**, 1753–1762.
21 P. Shieh, W. Zhang, K. E. L. Husted, S. L. Kristufek, B. Xiong, D. J. Lundberg, J. Lem, D. Veysset, Y. Sun, K. A. Nelson, D. L. Plata and J. A. Johnson, *Nature*, 2020, **583**, 542–547.
22 Z. Yao, L. Zhou, B. Dai and K. Cao, *J. Appl. Polym. Sci.*, 2012, **125**, 2489–2493.
23 A. David, J. Huang, E. Richaud and P. Y. Le Gac, *Polym. Degrad. Stab.*, 2020, **179**, 109294.
24 W. Callister Jr. and D. Rethwisch, *Materials Science and Engineering: An Introduction*, John Wiley & Sons, Inc, 9th edn, 2014.
25 H. Wu, F. Dave, M. Mokhtari, M. M. Ali, R. Sherlock, A. McIlhagger, D. Tormey and S. McFadden, *Polymers*, 2022, **14**, 1804.
26 P. Zhang, S. X. Li and Z. F. Zhang, *Mater. Sci. Eng., A*, 2011, **529**, 62–73.
27 B. Godwin, D. Bouetard, J. Talcik, A. Del Vecchio, F. Morvan, T. Roisnel, M. Mauduit and J. E. Wulff, *ACS Appl. Polym. Mater.*, 2024, **7**, 377–385.
28 I. Czelusniak, J. D. Heywood, A. M. Kenwright and E. Khosravi, *J. Mol. Catal. A: Chem.*, 2008, **280**, 29–34.
29 M. G. Hyatt, D. J. Walsh, R. L. Lord, J. G. Andino Martinez and D. Guironnet, *J. Am. Chem. Soc.*, 2019, **141**, 17918–17925.
30 D. J. Sutor, *J. Chem. Soc.*, 1963, **0**, 1105–1110.
31 D. J. Sutor, *Nature*, 1962, **195**, 68–69.
32 C. H. Schwalbe, *Cryst. Rev.*, 2012, **18**, 191–206.
33 Y. Mai and A. Eisenberg, *Chem. Soc. Rev.*, 2012, **41**, 5969–5985.
34 V. S. Kravchenko, V. Abetz and I. I. Potemkin, *Polymer*, 2021, **235**, 124288.
35 T. R. Long, R. M. Elder, E. D. Bain, K. A. Masser, T. W. Sirk, J. H. Yu, D. B. Knorr and J. L. Lenhart, *Soft Matter*, 2018, **14**, 3344–3360.
36 C. Nicolas, J. Huang, E. Richaud, A. David, P.-Y. Le Gac, W. Minne, R. Drozdzak, G. Recher, L. Fontaine and V. Montembault, *Polym. Degrad. Stab.*, 2022, **195**, 109765.